Incorporation of Mn^{III} and Fe^{II} Complexes into TCNQ Networks: Preparations, Crystal Structures, and Magnetic Properties of $[Mn^{III}(salen)(TCNQ)_{0.5}][Mn^{III}(salen)(TCNQ)_{0.5}(CH_3OH)]$-$CH_3OH\cdot H_2O$ and $[Fe^{II}(CH_3OH)_4(TCNQ)_2]TCNQ\cdot 2CH_3CN$

Hiroki Oshio,* Etsuo Ino, Tasuku Ito,* and Yonezo Maeda†

Department of Chemistry, Faculty of Science, Tohoku University, Aoba-ku, Sendai 980

†Department of Chemistry, Faculty of Science, Kyusyu University, Higashi-ku, Fukuoka 810

(Received September 29, 1994)

Metal complexes with TCNQ as ligands, $[Mn^{III}(salen)(TCNQ)_{0.5}][Mn^{III}(salen)(TCNQ)_{0.5}(CH_3OH)]$-$CH_3OH\cdot H_2O$ (**1**) and $[Fe^{II}(CH_3OH)_4(TCNQ)_2]TCNQ\cdot 2CH_3CN$ (**2**) (where TCNQ and H_2salen represent tetracyanoquinodimethane and quadridentate schiff base N,N'-disalicylideneethylenediamine, respectively) were prepared, and crystal structures and magnetic properties were studied. Complex **1** crystallizes in the triclinic space group $P\bar{1}$ with cell constants $a=12.000(6)$, $b=19.986(7)$, $c=9.494(6)$ Å, $\alpha=100.67(5)$, $\beta=100.01(5)$, $\gamma=81.50(4)°$, $V=2188(2)$ Å^3, and $Z=2$. In **1**, two distinct six-coordinate $[Mn^{III}(salen)]^+$ chromophores are bridged by two kinds of $TCNQ^{2-}$ anions (**A** and **B**) in μ_2 and μ_4 fashions to form a one-dimensional structure. Complex **2** crystallizes in the triclinic space group $P\bar{1}$ with cell constants $a=10.523(1)$, $b=14.008(2)$, $c=8.062(1)$ Å, $\alpha=94.96(1)$, $\beta=111.11(1)$, $\gamma=79.96(1)°$, $V=1091.3(3)$ Å^3, and $Z=1$. In **2**, mono-anionic and neutral TCNQ molecules (**C** and **D**, respectively) stacks to form columns (···**DCCD**···), which are linked by the coordination of the nitrile group to $[Fe^{II}(CH_3OH)_4]^{2+}$. Temperature dependent magnetic susceptibility measurements revealed that magnetic interactions between metal centers in **1** and **2** are very small.

Various kinds of molecular based magnetic materials have been currently investigated and some coordination and pure organic compounds were reported to show spontaneous magnetization at low temperature. Macroscopic properties like magnetic ordering or high-electric conductivity can be attained when constituent molecules have multi-dimensional interactions. Some inorganic salts with organic radicals like TCNQ (tetracyanoquinodimethane), TCNE (tetracyanoethylene), TTF (tetrathiafulvalene), and DCNQI (dicyanoquinonediimine) families, which have multidimentional networks in a solid, are organic metal or semi-conductor. If paramagnetic metal complexes are incorporated into such organic radical networks, interesting macroscopic properties like magnetic metal can be attained. Furthermore, information about which metal ions can propagate strong magnetic interactions with organic radicals is useful for designing such magnetic materials.

Metal complexes with TCNQ or TCNE families have been studied from the structural and magnetochemical view points. A series of metallocene–TCNQ and TCNE charge transfer complexes have been reported to have strong charge transfer interactions between metallocene and anion radicals, and this leads to strong magnetic interactions.1) $[M(C_5M_5)_2](TCNE)$ (M=Fe,2) Mn,3) Cr4)) and $[M(C_5Me_5)_2](TCNQ)$ (M=Fe,5) Mn,6) Cr7)) have shown a spontaneous magnetization below 10 K. It should be noted that $[V(TCNE)_x]\cdot y(CH_2Cl_2)$8) has been reported to be a room temperature magnet. From these experimental results, organometallics seems to have strong magnetic and electronic interactions with organic radicals.9) On the other hand, metal complexes (so-called Werner type complex) are very stable and easy to handle, and sometimes their redox properties can be controlled by modifications of the ligands. However, structurally characterized TCNQ compounds with such Werner type complexes have not shown strong magnetic interactions even when the TCNQ radicals coordinate directly to central metal ions. For examples, $[M(abpt)_2(TCNQ)]$ (M=Cu^{II}, Ni^{II}, Co^{II}),10) $[Cu_2(L)(TCNQ)_2]$,11) and $[Mn^{II}(tpa)(TCNQ)(CH_3OH)](TCNQ)_2\cdot CH_3CN$12) (abpt=3,5-bis(pyridin-2-yl)-4-amino-1,2,4-triazole, L = a tetra-Schiff base macrocycle resulting from the 2/2 condensation of 1,3-dimaninopropane and 2,6-diformyl-4-methylphenol, and tpa=tris(2-pyridylmethyl)amine) were reported to have fairly weak or no magnetic interactions between paramagnetic species. Coordination compounds with

$Mn^{II}(d^5)$, $Co^{II}(d^7)$ and $Ni^{II}(d^8)$ ions seems not to be good candidates for network constituents to achieve macroscopic properties in solids. In this paper, we report crystal structures and magnetic properties of TCNQ compounds with $Mn^{III}(d^4)$ and $Fe^{II}(d^6)$ complexes as network constituents.

Experimental

General Procedures. All chemicals were reagent grade and were used as received. Methanol and acetonitrile were distilled over sodium and calcium hydride, respectively, under N_2. LiTCNQ and schiff-base ligand (H_2salen), and $[Mn^{III}(salen)](PF_6)\cdot H_2O$ were prepared by the literature methods.[13] All procedures were carried out under N_2 atmosphere using Schlenk technique.

Preparation of $[Mn^{III}(salen)(TCNQ)_{0.5}][Mn^{III}(salen)(TCNQ)_{0.5}(CH_3OH)]CH_3OH\cdot H_2O$ (1). $[Mn^{III}(salen)](PF_6)\cdot H_2O$ (117 mg, 0.25 mmol), dissolved in 30 mL of acetonitrile, was added to a solution of LiTCNQ (53 mg, 0.25 mmol) in 10 mL of methanol. The resulting dark greenish mixture was stirred for 1 h and concentrated to 30 mL. On standing for 2 weeks in a refrigerator, the resulting dark red crystalline was filtered and washed with cold methanol, and one of them was subjected to an X-ray structural analysis. Anal. Calcd for $C_{46}H_{42}Mn_2N_8O_7$: C, 59.49; H, 4.56; N, 12.06%. Found: C, 59.30; H, 4.47; N, 11.99%.

Preparation of $[Fe^{II}(CH_3OH)_4(TCNQ)_2]TCNQ\cdot 2CH_3CN$ (2). A solution of $Fe(NO_3)_3\cdot 9H_2O$ (81 mg, 0.20 mmol) and H_2salen (54 mg, 0.20 mmol) in 30 mL of acetonitrile was added to a solution of LiTCNQ (43 mg, 0.20 mmol) in 10 mL of MeOH. The resulting dark blue solution was stirred for 1 h. Filtrate was concentrated to 30 mL. After standing for 3 d in refrigerator, black crystals were filtrated and washed with cold methanol. It should be noted that attempt to prepare **2** using iron(II) chloride and LiTCNQ in methanol was unsuccessful, however. Anal. Calcd for $C_{44}H_{34}FeN_{14}O_4$: C, 60.14; H, 3.90; N, 22.32%. Found: C, 59.91; H, 3.69; N, 22.22%.

Magnetic Measurement. Magnetic susceptibility data were collected in the temperature range 2.0—300 K and in applied 0.1 Tesla with the use of a Quantum Design Model MPMS SQUID magnetometer. Powdered samples were contained in the small half of a gelatin capsule and a phenolic guide (clear soda straw) was used to house the sample holder and was fixed to the end of the magnetometer drive rod. $[Cr(NH_3)_6](NO_3)_3$ was employed as dual magnetometer calibrants. Pascal's constants were used to determine the constituent atom diamagnetism.[14]

Mössbauer and IR Spectroscopic Measurements. Mössbauer spectrum was measured with a constant-acceleration spectrometer (Austin Science Associates) at 287 K. Data were stored in a 1024-channel pulse-height analyzer, type 5200 (Inotech, Inc). A ^{57}Co (10 mCi) diffused into a palladium foil was used as a source. Spectrum was analyzed with a pair of Lorentzian lines using a least-squares fitting procedure. The velocity scale was normalized with respect to the centre of the spectrum of metallic iron at 296 K. IR spectra were measured on a Bruker IFS66v FT-IR spectrophotometer using Nujol mulls technique.

Electrochemical Methods. Cyclic voltammetry (CV) measurements were accomplished with a three-electrode potentiostat (Hokuto Denko HA501G potentiostat/galvanostat and HB-105 function generator). The internal resistance drop was compensated with a Hokuto HI-203 IR compensation instrument for CV. The electrochemical measurements were performed at 25 °C by the use of a normal three electrode configuration consisting of a highly polished glassy carbon working electrode (area 0.28 cm^3; BAS Ltd.), a platinum-wire auxiliary electrode, and an $Ag-Ag^+$ reference electrode containing 0.01 $mol\,dm^{-3}$ $AgNO_3$ and 0.1 $mol\,dm^{-3}$ tetrabutylammonium perchlorate (TBAP) acetonitrile solution (BAS Ltd.) in a micro-cell. The working and auxiliary compartments contained a 0.1 $mol\,dm^{-3}$ solution of the supporting electrolyte. Spectral grade acetonitrile (Dojin Lab.) was used without further purification. The supporting electrolyte TBAP was recrystallized two times from ethanol and water, and dried under vacuum for 12 h. The compartment of the cell was bubbled with solvent-saturated argon to deaerate the solution. The reference electrode was checked periodically against the ferrocenium/ferrocene couple (Fc^+/Fc) in acetonitirle. The half-wave potential of Fc^+/Fc under the condition employed was 0.12 V ($\Delta E_p = 70$ mV) vs. Ag/Ag^+. Potentials for the compounds are reported relative to the Ag/Ag^+ reference electrode.

X-Ray Crystallography. A single crystal for **1** and **2** were mounted on the tips of glass fibers with epoxy resin and coated with epoxy resin to prevent possible solvent loss. Diffraction data were collected on a Rigaku 7S four circle diffractometer equipped with liquid N_2 cryostream cooler (Oxford Cryosystems). Graphite monochromatized Mo $K\alpha$ radiation ($\lambda = 0.71069$ Å) was used for the measurement. All data were collected for Lorentz and polarization effects and empirical absorption corrections (Ψ-scans) were carried out in each case. No decay in intensity was observed during measurements. The lattice constants were optimized from a least-squares refinement of the settings of 25 carefully centered Bragg reflections in the range of $25° < 2\theta < 30°$. Crystallographic data were collected in Table 1. The structures were solved by the direct method with SHELEX-86[15] and Fourier techniques, and refined by the full-matrix least-squares method using XTAL 3.2.[16] All non-hydrogen atoms were readily located and refined with anisotropic thermal parameters. Hydrogen atoms were located from difference Fourier maps. Positional and thermal parameters of hydrogen atoms for **1** were fixed, while those for **2** were refined with isotropic thermal parameters. Final atomic parameters and equivalent isotropic thermal parameters for non-hydrogen atoms are listed in Tables 2 and 3. The complete F_o-F_c data are deposited as Document No. 68012 at the Office of the Editor of Bull. Chem. Soc. Jpn.

Results and Discussion

Spectroscopic Data. Infrared spectroscopic studies have demonstrated that vibrational frequencies provide significant information on charges of TCNQ molecules.[17] Especially, nitrile groups give characteristic ν_{CN} stretching frequencies (2000—2250 cm^{-1}) depending on the nature of the TCNQ molecules. Bands above 2200 cm^{-1} were assigned to the CN stretching for $TCNQ^0$ molecules,[18] while bands be-

Table 1. Crystal and Refinement Data for $[Mn(salen)(TCNQ)_{0.5}][Mn(salen)(TCNQ)_{0.5}(CH_3OH)]CH_3OH{\cdot}H_2O$ (**1**) and $[Fe(CH_3OH)_4(TCNQ)_2]TCNQ{\cdot}2CH_3CN$ (**2**)

Formula	$C_{46}H_{42}Mn_2N_8O_7$	$C_{44}H_{34}FeN_{14}O_4$
FW	928.77	878.69
Temperature/K	293	173
Crystal system	Triclinic	Triclinic
Space group	$P\bar{1}$	$P\bar{1}$
a/Å	12.000(6)	10.523(1)
b/Å	19.986(7)	14.008(2)
c/Å	9.494(6)	8.062(1)
α/°	100.67(5)	94.96(1)
β/°	100.01(5)	111.11(1)
γ/°	81.50(4)	79.96(1)
V/Å^3	2188(2)	1091.3(3)
Z	2	1
D_{calcd}/g cm^{-3}	1.410	1.337
Radiation(Mo $K\alpha$)/Å	0.71069	0.71069
μ(Mo $K\alpha$)/cm^{-1}	3.057	4.004
Total data collected	7669	4085
Independent data, $\lvert F_o \rvert > 6\sigma(F_o)$	4745	3469
Transmision coeff.	0.830—0.87	0.881—1.00
$R^{a)}$	0.060	0.030
$R_w{}^{b)}$	0.088	0.045

a) $R=\Sigma(|F_o|-|F_c|)/\Sigma|F_o|$. b) $R_w[\Sigma w(|F_o|-|F_c|)^2/\Sigma w|F_o|^2]^{1/2}$, c) $w=(\sigma_c^2+(0.020\times|F_o|)^2)^{-1}$.

low 2200 cm^{-1} are due to the TCNQ$^-$ anion.[7] TCNQ^{2-} in Na_2TCNQ shows ν_{CN} bands at 2150 and 2096 cm^{-1}.[19] The absorptions at 2065 (sh), 2100, and 2113 cm^{-1} in $[Mn^{III}(salen)(TCNQ)_{0.5}][Mn^{III}(salen)(TCNQ)_{0.5}(CH_3OH)]CH_3OH{\cdot}H_2O$ (**1**) are a clear indication that the TCNQ^{2-} anions are present. $[Fe^{II}(CH_3OH)_4(TCNQ)_2]TCNQ{\cdot}2CH_3CN$ (**2**) shows ν_{CN} stretching bands at 2156, 2174, 2195, 2211, and 2225 (sh) cm^{-1}, which are characteristic of TCNQ^0 and TCNQ$^-$ molecules. The splitting of the ν_{CN} bands can be explained by assuming that the nitrile groups are inequivalent, e.g. coordination or uncoordination to the metal ions.

The Mössbauer spectrum of a polycrystalline sample of **2** at 293 K consisted of a single quadrupole doublet. An isomer shift (δ) of 1.09 mm s^{-1} is characteristic of high-spin iron(II) ions. The quadrupole splitting parameter (ΔE_Q) of 3.17 mm s^{-1} indicates a unsymmetrical electric field, consistent with the elongated octahedral coordination about the iron ion.

Description of the Structure. $[Mn^{III}(salen)(TCNQ)_{0.5}][Mn^{III}(salen)(TCNQ)_{0.5}(CH_3OH)]CH_3OH{\cdot}H_2O$ (1). An ORTEP drawing with numbering scheme of **1** is shown in Fig. 1. Selected bond lengths and angles about manganese ions are listed in Table 4. Complex **1** crystallizes in the triclinic space group $P\bar{1}$. The dark red crystal consists of two kinds of crystallographically independent [Mn(salen)] and TCNQ molecules (called **A** and **B**), where TCNQ molecules are locating on inversion centre. The cations [Mn(salen)] are mono-ionic, therefore the TCNQ molecules are di-anionic (TCNQ^{2-}). TCNQ^{2-} in **1** show quite different intramolecular bond lengths from those of TCNQ$^-$. Intramolecular bond distances of TCNQ molecules reflect their electronic nature. Selected intramolecular bond distances of TCNQ are listed in Table 6 together with bond notations and scheme of the lowest unoccupied molecular orbital (LUMO) of TCNQ. As negative charges on TCNQ molecules increased, bonds **a** and **c** with antibonding character are lengthen, while bonds **b** and **d** with bonding character are reversed.[11] Bonds **a** (1.371—1.380 Å) and **c** (1.481—1.491 Å) for **A** and **B** are longer than those (1.358—1.375 Å and 1.405—1.438 Å) for other TCNQ^{-1}. Bonds **b** (1.38—1.395 Å) and **d** (1.37—1.392 Å) for **A** and **B** are shorter than those (1.406—1.425 Å and 1.40—1.48 Å) for the TCNQ^{-1} anions. Manganese ions have a six-coordination geometry and an equatorial plane consists of two N and two O atoms of salen, of which Mn1 and Mn2 ions are displaced by 0.064(1) and 0.116(1) Å above N_2O_2 plane. Two axial positions of Mn1 are occupied by the two N atoms from TCNQ^{2-} (**A** and **B**). Mn2 are coordinated by one N atom of TCNQ^{2-} (**B**) and one O atom of methanol. Two N atoms (N5) of **A** bridge two of Mn1 ions, while **B** bridges two of Mn1 and Mn2 ions through the coordination of four N atoms (N7 and N8). Hence, TCNQ^{2-} (**A** and **B**) act as bridging ligand with μ_2- and μ_4-fashions, respectively, to form one-dimensional structure (Fig. 2). Separations of manganese ions by TCNQ^{2-} ions were

Table 2. Fractional Coordinates and Equivalent Isotropic Displacement Parameters ($Å^2$) of Non-Hydrogen Atoms of $[Mn(salen)(TCNQ)_{0.5}][Mn(salen)(TCNQ)_{0.5}(CH_3OH)]CH_3OH{\cdot}H_2O$ (**1**)

Atom	x/a	y/b	z/c	$U^{a)}$	Atom	x/a	y/b	z/c	$U^{a)}$
Mn(1)	0.17426(8)	0.31868(6)	0.9684(1)	0.0308(4)	C(16)	0.4632(6)	0.3740(4)	1.2427(8)	0.046(3)
Mn(2)	0.63402(9)	0.18623(5)	0.6159(1)	0.0338(4)	C(17)	0.7669(7)	0.0689(4)	0.4728(8)	0.045(3)
O(1)	0.2185(4)	0.2907(3)	0.7832(5)	0.040(2)	C(18)	0.8478(7)	0.0429(5)	0.3798(9)	0.059(3)
O(2)	0.3204(4)	0.3299(3)	1.0637(5)	0.041(2)	C(19)	0.8697(8)	−0.0272(5)	0.331(1)	0.074(4)
O(3)	0.7478(4)	0.1357(2)	0.5153(6)	0.049(2)	C(20)	0.8136(9)	−0.0728(5)	0.375(1)	0.075(4)
O(4)	0.6734(4)	0.2706(2)	0.5961(5)	0.044(2)	C(21)	0.7372(9)	−0.0511(4)	0.465(1)	0.073(4)
O(5)	−0.2359(5)	0.1939(3)	0.8384(6)	0.057(2)	C(22)	0.7096(7)	0.0205(4)	0.5200(8)	0.052(3)
O(6)	−0.2925(7)	0.2589(3)	1.0913(7)	0.086(3)	C(23)	0.6317(7)	0.0418(4)	0.6220(9)	0.053(3)
O(7)	0.101(2)	0.058(1)	1.109(2)	0.19(1)	C(24)	0.5252(8)	0.1177(5)	0.7896(9)	0.063(4)
N(1)	0.0131(4)	0.3067(3)	0.8872(6)	0.036(2)	C(25)	0.4507(7)	0.1827(4)	0.7760(9)	0.053(3)
N(2)	0.1102(4)	0.3356(3)	1.1520(6)	0.033(2)	C(26)	0.5093(6)	0.2943(4)	0.8026(7)	0.038(3)
N(3)	0.5968(5)	0.1028(3)	0.6741(7)	0.044(2)	C(27)	0.6553(6)	0.3304(4)	0.6813(7)	0.036(2)
N(4)	0.5208(5)	0.2301(3)	0.7429(6)	0.037(2)	C(28)	0.5758(6)	0.3446(4)	0.7800(7)	0.039(3)
N(5)	0.1400(6)	0.4296(3)	0.9463(7)	0.047(2)	C(29)	0.5620(7)	0.4114(4)	0.8624(8)	0.052(3)
N(6)	0.2877(5)	0.6004(4)	0.8204(7)	0.057(3)	C(30)	0.6241(9)	0.4609(4)	0.8515(9)	0.062(4)
N(7)	0.4982(6)	0.1710(3)	1.4118(7)	0.051(3)	C(31)	0.7024(8)	0.4468(4)	0.7560(9)	0.056(3)
N(8)	0.2273(6)	0.1949(4)	1.0314(7)	0.053(3)	C(32)	0.7183(6)	0.3832(4)	0.6716(8)	0.045(3)
C(1)	0.1592(6)	0.2658(4)	0.6600(7)	0.037(3)	C(33)	0.1504(6)	0.4662(4)	0.8697(7)	0.039(3)
C(2)	0.2127(6)	0.2463(4)	0.5349(7)	0.043(3)	C(34)	0.1568(6)	0.5083(4)	0.7704(7)	0.037(2)
C(3)	0.1568(7)	0.2167(4)	0.4047(8)	0.054(3)	C(35)	0.2311(6)	0.5567(4)	0.8017(7)	0.041(3)
C(4)	0.0454(8)	0.2051(5)	0.3931(8)	0.059(4)	C(36)	0.0767(6)	0.5033(3)	0.6324(7)	0.034(2)
C(5)	−0.0119(7)	0.2246(4)	0.5079(8)	0.050(3)	C(37)	−0.0067(6)	0.4594(4)	0.5991(8)	0.043(3)
C(6)	0.0434(6)	0.2550(4)	0.6440(7)	0.037(2)	C(38)	0.0809(6)	0.5440(4)	0.5286(7)	0.039(3)
C(7)	−0.0247(6)	0.2781(4)	0.7589(8)	0.037(3)	C(39)	0.4526(6)	0.1532(4)	1.2947(8)	0.038(3)
C(8)	−0.0662(6)	0.3342(4)	0.9909(8)	0.047(3)	C(40)	0.4005(6)	0.1282(4)	1.1559(7)	0.039(3)
C(9)	−0.0081(6)	0.3185(4)	1.1328(7)	0.042(3)	C(41)	0.3052(7)	0.1654(4)	1.0894(7)	0.041(3)
C(10)	0.1615(6)	0.3602(4)	1.2763(7)	0.037(3)	C(42)	0.4517(6)	0.0622(3)	1.0779(6)	0.033(2)
C(11)	0.3514(5)	0.3582(3)	1.2010(7)	0.034(2)	C(43)	0.5649(6)	0.0356(4)	1.1156(7)	0.035(2)
C(12)	0.2776(6)	0.3748(3)	1.3074(7)	0.033(2)	C(44)	0.3880(6)	0.0246(4)	0.9603(7)	0.038(3)
C(13)	0.3202(7)	0.4050(4)	1.4489(7)	0.046(3)	C(45)	−0.142(1)	0.1433(6)	0.870(1)	0.103(6)
C(14)	0.4277(7)	0.4212(4)	1.4856(8)	0.054(3)	C(46)	−0.307(1)	0.2249(6)	1.206(1)	0.099(6)
C(15)	0.5000(6)	0.4044(5)	1.3802(9)	0.055(3)					

a) Equivalent isotropic U defined as one-third of the trace of the orthogonalized U_{ij} tensor.

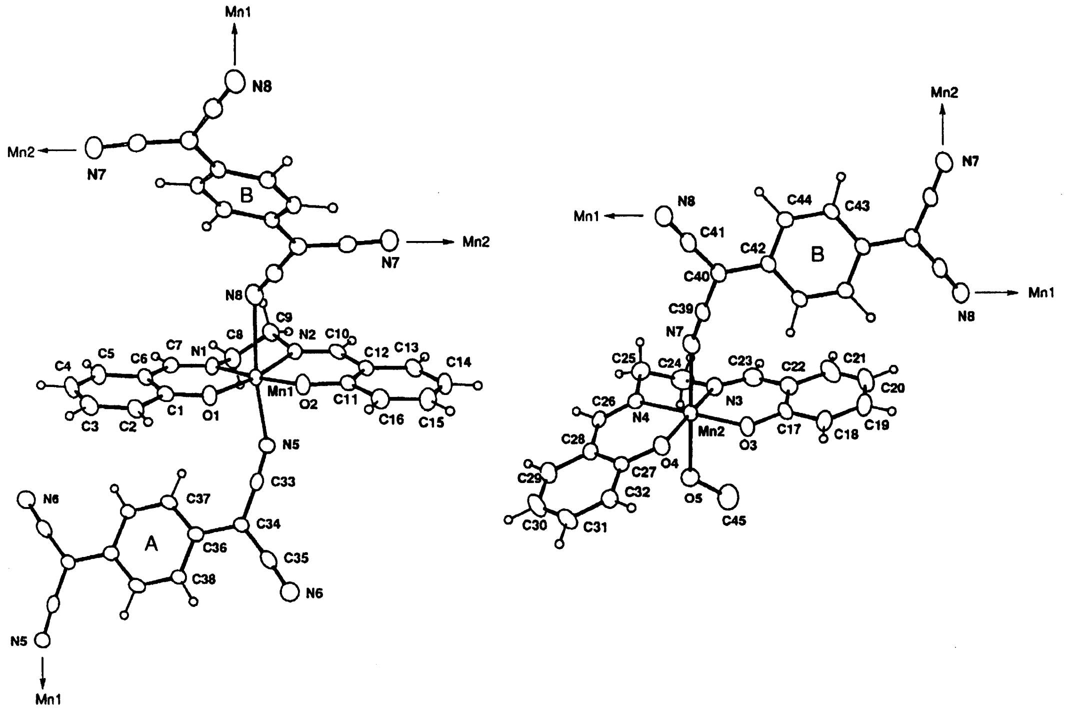

Fig. 1. ORTEP drawings of $[Mn^{III}(salen)(TCNQ)_{0.5}][Mn^{III}(salen)(TCNQ)_{0.5}(CH_3OH)]$ (**1**).

Table 3. Fractional Coordinates and Equivalent Isotropic Displacement Parameters (Å^2) of Non-Hydrogen Atoms of [Fe(CH$_3$OH)$_4$(TCNQ)$_2$]-TCNQ·2CH$_3$CN (**2**)

Atom	*x*/*a*	*y*/*b*	*z*/*c*	$U^{a)}$
Fe	1/2	1/2	1/2	0.0190(1)
O(1)	0.6142(1)	0.43344(9)	0.3407(2)	0.0335(5)
O(2)	0.6758(1)	0.46494(9)	0.7234(1)	0.0287(4)
N(1)	0.4341(1)	0.36855(9)	0.5249(2)	0.0253(5)
N(2)	0.3125(2)	0.2236(1)	0.8924(2)	0.0392(6)
N(3)	0.3458(2)	−0.1119(1)	−0.1650(2)	0.0345(6)
N(4)	0.2579(2)	−0.2714(1)	0.2082(2)	0.0324(6)
N(5)	0.9820(2)	0.1595(1)	0.5299(2)	0.0431(7)
N(6)	1.0542(2)	0.3295(1)	0.1605(2)	0.0473(7)
N(7)	1.1758(2)	0.4737(1)	0.6608(2)	0.0447(7)
C(1)	0.3547(1)	0.1337(1)	0.4878(2)	0.0186(5)
C(2)	0.3699(2)	0.1354(1)	0.3193(2)	0.0197(5)
C(3)	0.3605(2)	0.0557(1)	0.2095(2)	0.0199(5)
C(4)	0.3357(1)	−0.0327(1)	0.2584(2)	0.0189(5)
C(5)	0.3192(2)	−0.0341(1)	0.4258(2)	0.0203(5)
C(6)	0.3284(2)	0.0456(1)	0.5359(2)	0.0202(5)
C(7)	0.3652(2)	0.2165(1)	0.6029(2)	0.0200(5)
C(8)	0.4013(2)	0.3011(1)	0.5601(2)	0.0203(5)
C(9)	0.3370(2)	0.2203(1)	0.7639(2)	0.0247(6)
C(10)	0.3252(2)	−0.1150(1)	0.1433(2)	0.0208(5)
C(11)	0.3384(2)	−0.1134(1)	−0.0262(2)	0.0230(6)
C(12)	0.2899(2)	−0.2015(1)	0.1811(2)	0.0225(5)
C(13)	1.0275(2)	0.0855(1)	−0.0523(2)	0.0240(6)
C(14)	1.0074(2)	0.0829(1)	0.1155(2)	0.0231(6)
C(15)	1.0195(2)	0.0070(1)	−0.1613(2)	0.0240(6)
C(16)	1.0138(2)	0.1628(1)	0.2276(2)	0.0255(6)
C(17)	1.0373(2)	0.2546(1)	0.1880(2)	0.0305(6)
C(18)	0.9958(2)	0.1603(1)	0.3954(2)	0.0293(6)
C(19)	0.6400(3)	0.3345(2)	0.2855(3)	0.0465(9)
C(20)	0.7101(3)	0.5154(2)	0.8914(3)	0.0512(9)
C(21)	0.9942(2)	0.3938(2)	0.7215(3)	0.0481(9)
C(22)	1.0958(2)	0.4380(1)	0.6857(2)	0.0333(7)

a) Equivalent isotropic *U* defined as one-third of the trace of the orthogonalzed U_{ij} tensor.

Table 4. Bond Distance (Å) and Angles (°) of [Mn(salen)(TCNQ)$_{0.5}$][Mn(salen)(TCNQ)$_{0.5}$(CH$_3$OH)]CH$_3$OH·H$_2$O (**1**)

Mn1–O1	1.887(5)	Mn1–O2	1.853(4)
Mn1–N1	1.986(5)	Mn1–N2	1.979(6)
Mn1–N5	2.235(7)	Mn1–N8	2.615(7)
Mn2–O3	1.867(5)	Mn2–O4	1.866(5)
Mn2–O5	2.393(5)	Mn2–N3	1.983(7)
Mn2–N4	1.973(6)	Mn2–N7	2.310(6)
Mn1–Mn1^{*1}	12.294(5)	Mn1–Mn1^{*2}	13.981(4)
Mn2–Mn2^{*3}	12.818(6)	Mn1–Mn2^{*4}	8.072(3)
Mn1–Mn2^{*5}	10.071(3)		
O1–Mn1–O2	94.8(2)	O1–Mn1–N1	91.1(2)
O1–Mn1–N2	170.1(2)	O1–Mn1–N5	93.9(2)
O1–Mn1–N8	92.1(2)	O2–Mn1–N1	173.8(2)
O2–Mn1–N2	92.7(2)	O2–Mn1–N5	91.2(2)
O2–Mn1–N8	83.0(2)	N1–Mn1–N2	81.2(2)
N1–Mn1–N5	90.1(2)	N1–Mn1–N8	95.0(2)
N2–Mn1–N5	92.3(2)	N2–Mn1–N8	82.5(2)
N5–Mn1–N8	172.0(2)	O3–Mn2–O4	93.6(2)
O3–Mn2–O5	90.8(2)	O3–Mn2–N3	91.9(2)
O3–Mn2–N4	171.5(2)	O3–Mn2–N7	91.5(2)
O4–Mn2–O5	87.2(2)	O4–Mn2–N3	169.9(2)
O4–Mn2–N4	92.5(2)	O4–Mn2–N7	98.6(2)
O5–Mn2–N3	84.3(2)	O5–Mn2–N4	83.6(2)
O5–Mn2–N7	173.6(2)	N3–Mn2–N4	81.3(3)
N3–Mn2–N7	89.7(2)	N4–Mn2–N7	93.4(2)
Mn1–N5–C33	140.7(5)	Mn1–N8–C41	135.9(6)
Mn2–N7–C39	162.9(6)		
	TCNQ **A**		
N5–C33	1.16(1)	N6–C35	1.15(1)
C33–C34	1.39(1)	C34–C35	1.37(1)
C34–C36	1.481(9)	C36–C37	1.38(1)
C36–C38	1.40(1)	C37–C38	1.371(9)
N5–C33–C34	176.0(7)	C33–C34–C35	121.3(6)
C33–C34–C36	119.1(6)	C35–C34–C36	119.6(7)
N6–C35–C34	174.5(8)	C34–C36–C37	122.6(7)
C34–C36–C38	121.1(6)	C37–C36–C38	116.4(6)
C36–C37–C38	121.7(8)	C36–C38–C37	121.9(7)
	TCNQ **B**		
N7–C39	1.167(9)	N8–C41	1.14(1)
C39–C40	1.392(9)	C40–C41	1.39(1)
C40–C42	1.491(9)	C42–C43	1.395(9)
C42–C44	1.399(9)	C43–C44	1.380(9)
N7–C39–C40	176.7(8)	C39–C40–C41	120.5(6)
C39–C40–C42	118.8(6)	C41–C40–C42	120.7(6)
N8–C41–C40	178.2(7)	C40–C42–C43	122.2(5)
C40–C42–C44	121.0(6)	C43–C42–C44	116.8(6)
C42–C43–C44	121.5(6)	C42–C44–C43	121.7(6)

* Key to symmetry operations; ^{1}: $-x$, $1-y$, $1-z$; ^{2}: $1-x$, $-y$, $2-z$; ^{3}: $1-x$, $-y$, $-z$; ^{4}: x, y, $1+z$; ^{5}: $-1-x$, $-y$, $1-z$.

listed in Table 4. Bond distances between manganese atom and coordinated atoms are 1.853(4)—1.979(6) Å for equatorial and 2.235(7)—2.615(7) Å for axial atoms. The elongated octahedral geometry around the manganese ions are due to the Jahn–Teller distortion of the manganese ions. Mn–NCC (TCNQ^{2-}) linkages are not collinear (Mn–N–C angles are 135.9(6)—162.9°) in comparison with the TCNQ$^-$ coordination. Fe–NCC (TCNQ$^-$) linkages in **2** is essentially collinear with the iron-nitrogen bond (Fe–N1–C8=171.5°). The nonlinear linkage in **1** can be understood by the fact of the weakened CN bond in TCNQ^{2-}. The CN bond in TCNQ has antibonding character in the LUMO, so the nitrile triple bond is weakened as the negative charges on TCNQ molecules increased. Bond lengths of CN groups for TCNQ^{2-} (1.14—1.167 Å) are rather long compared with those (1.126—1.156 Å) of TCNQ$^-$. It is reasonable to suppose that the nitrile group in TCNQ^{2-} slightly have double bond character and the coordinating nitrogen atoms tend to coordinate to the metal ion in sp^2 fashion. Hence, the M-NCC linkage is not collinear for the coordination of TCNQ^{2-}.

[Fe^{II}(CH$_3$OH)$_4$(TCNQ)$_2$]TCNQ·2CH$_3$CN (2).

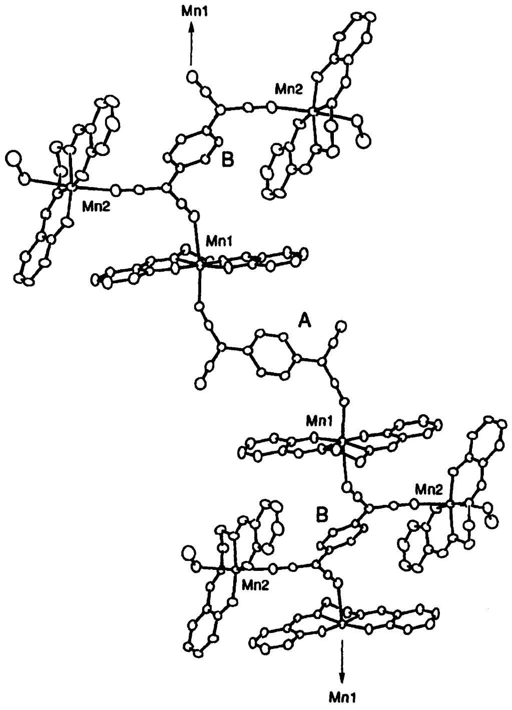

Fig. 2. One dimensional structure of $[Mn^{III}(salen)(TCNQ)_{0.5}][Mn^{III}(salen)(TCNQ)_{0.5}(CH_3OH)]$ (**1**).

The structure of **2** is shown in Fig. 3, and bond length and angles relevant to the iron coordination sphere are given in Table 5. The crystal consist of iron(II) chromophore and two kinds of crystallographically independent TCNQ molecules (**C** and **D**), where the iron(II) chromophore and TCNQ (**D**) molecule locate on the center of symmetry. The iron(II) ion is bound in an elongated octahedral fashion. Four O atoms from methanol and two N atoms from TCNQ (**C**) occupy the equatorial and axial sites, respectively. Bond distances between iron and coordinating atoms are 2.087(1)—2.118(2) Å for the equatorial O atoms and 2.127(2) Å for the axial N atoms. Comparison of the intramolecular bond lengths in **C** and **D** with reported values for $TCNQ^0$ or $TCNQ^-$ leads to conclude that **C** and **D** are $TCNQ^-$ and $TCNQ^0$ molecules, respectively (Table 6). TCNQ molecules stack to form a column (···**DCCD**···), which are linked by the coordination of the nitrile groups to the iron(II) chromophores. **CC** and **CD** stacks in a ring–ring overlap (R–R) and a ring–external bond overlap (R–B) modes,[20] respectively (Fig. 4). Interplaner distances between two **C**s is in the range 3.20—3.22 Å and that between **C** and **D** is 3.26—3.38 Å.

Electrochemistry. Redox properties of TCNQ, $[Mn^{III}(salen)](PF_6)\cdot H_2O$, and $[Fe^{III}(salen)Cl]$ were studied by the cyclic voltammetry. TCNQ molecule in acetonitrile show reversible redox waves at −0.11 V (vs. Ag/Ag^+) and −0.66 V which correspond to

Table 5. Bond Distance (Å) and Angles (°) of $[Fe(CH_3OH)_4(TCNQ)_2]TCNQ\cdot 2CH_3CN$ (**2**)

Fe–O1	2.118(2)	Fe–O2	2.087(1)
Fe–N1	2.127(2)		
O1–Fe–O2	88.16(5)	O1–Fe–N1	93.18(6)
O1–Fe–O2	91.84(5)	O1–Fe–N1	86.82(6)
O2–Fe–N1	89.33(5)	O2–Fe–N1	90.67(5)
Fe–N1–C8	171.5(1)		
	TCNQ C		
N1–C8	1.151(2)	N2–C9	1.150(3)
N3–C11	1.152(3)	N4–C12	1.151(2)
C1–C2	1.427(2)	C1–C6	1.424(2)
C1–C7	1.415(2)	C2–C3	1.358(2)
C3–C4	1.424(2)	C4–C5	1.424(3)
C4–C10	1.410(2)	C5–C6	1.359(2)
C7–C8	1.411(2)	C7–C9	1.428(3)
C10–C11	1.426(3)	C10–C12	1.416(2)
C2–C1–C6	117.6(1)	C2–C1–C7	121.3(2)
C6–C1–C7	121.2(2)	C1–C2–C3	121.1(2)
C2–C3–C4	121.3(2)	C3–C4–C5	117.5(1)
C3–C4–C10	121.1(2)	C5–C4–C10	121.4(2)
C4–C5–C6	121.3(2)	C1–C6–C5	121.2(2)
C1–C7–C8	120.8(2)	C1–C7–C9	122.6(2)
C8–C7–C9	116.6(1)	N1–C8–C7	178.1(2)
N2–C9–C7	179.1(2)	C4–C10–C11	121.7(2)
C4–C10–C12	122.6(2)	C11–10–C12	115.5(1)
N3–C11–C10	178.4(2)	N4–C12–C10	178.2(1)
	TCNQ D		
N5–C18	1.146(3)	N6–C17	1.146(3)
C13–C14	1.447(3)	C13–C15	1.342(2)
C14–C16	1.373(2)	C14–C15	1.443(3)
C16–C17	1.435(3)	C16–C18	1.436(3)
C14–C13–C15	120.6(2)	C13–C14–C16	121.4(2)
C13–C14–C15	117.7(1)	C16–C14–C15	120.9(2)
C13–C15–C14	121.7(2)	C14–C16–C17	123.6(2)
C14–C16–C18	121.6(2)	C17–C16–C18	114.8(1)
N6–C17–C16	177.6(2)	N5–C18–C16	179.0(2)

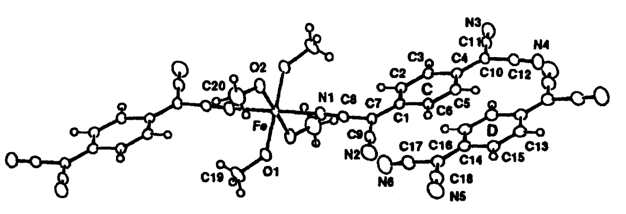

Fig. 3. ORTEP drawings of $[Fe^{II}(CH_3OH)_4(TCNQ)_2]TCNQ$ (**2**).

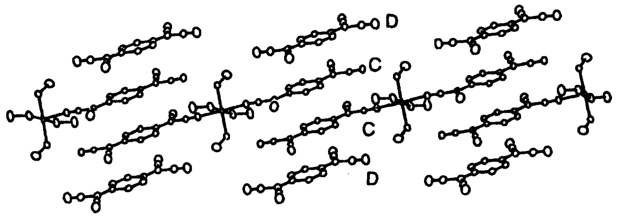

Fig. 4. Two demensional structure of $[Fe^{II}(CH_3OH)_4(TCNQ)_2]TCNQ$ (**2**).

Table 6. Bond Distances (Å) of TCNQ Molecules in $[Mn^{III}(salen)(TCNQ)_{0.5}]$-$[Mn^{III}(salen)(TCNQ)_{0.5}(CH_3OH)]CH_3OH{\cdot}H_2O$ (**1**), $[Fe^{II}(CH_3OH)_4(TCNQ)_2]$-$TCNQ{\cdot}2CH_3CN$ (**2**), and Related Complexes

	a	**b**	**c**	**d**	**e**
$[TCNQ]^0$ [a)]	1.330 │ 1.37	1.436 │ 1.453	1.34 │ 1.388	1.415 │ 1.433	1.126 │ 1.19
$[TCNQ]^-$ [b)]	1.358 │ 1.375	1.40 │ 1.425	1.405 │ 1.438	1.40 │ 1.48	1.126 │ 1.156
$[TCNQ]^{-2}$ **A** in **1**	1.380(9)	1.395(9)	1.491(9)	1.392(9) 1.39(1)	1.167(9) 1.14(1)
$[TCNQ]^{-2}$ **B** in **1**	1.371(9)	1.38(1)	1.481(9)	1.39(1) 1.37(1)	1.16(1) 1.15(1)
$[TCNQ]^{-1}$ **C** in **2**	1.361(4) 1.364(1)	1.421(3) 1.421(4) 1.422(4) 1.419(2)	1.415(3) 1.412(3)	1.415(3) 1.425(2) 1.421(4) 1.426(4)	1.149(3) 1.150(2) 1.149(5) 1.148(2)
$[TCNQ]^0$ **D** in **2**	1.339(4)	1.445(3) 1.441(4)	1.374(4)	1.439(3) 1.441(1)	1.140(6) 1.142(3)

a) Ref. 22. b) Refs. 10, 12, 16c, 18, and 23.

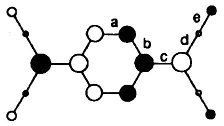

$TCNQ^0/TCNQ^-$ and $TCNQ^-/TCNQ^{2-}$ waves, respectively. $[Mn^{III}(salen)](PF_6){\cdot}H_2O$ show quasi-reversible and irreversible waves at −0.49 (ΔE_p=100 mV, Mn^{III}/Mn^{II}) and 1.2 V (Mn^{IV}/Mn^{III}), respectively, where ΔE_p is peak to peak separation. $[Fe^{III}(salen)Cl]$ show only quasi-reversible wave at −0.68 V (ΔE_p=100 mV, Fe^{III}/Fe^{II}). $[Mn^{III}(salen)(TCNQ)_{0.5}]$-$[Mn^{III}(salen)(TCNQ)_{0.5}(CH_3OH)]CH_3OH{\cdot}H_2O$ (**1**), which was prepared from $[Mn^{III}(salen)]^+$ and $TCNQ^-$, has $TCNQ^{2-}$ molecule. Formation of $TCNQ^{2-}$ ion is theoretically not probable from the view point of redox potentials. Therefore, $TCNQ^{2-}$ might be formed by one of the two ways. (i) Electron transfer between two of the coordinating $TCNQ^-$ anions through Mn^{III} ions results in formation of $TCNQ^0$ and $TCNQ^{2-}$ and only $TCNQ^{2-}$ crystallized with $[Mn^{III}(salen)]^+$ cation. (ii) The coordinating $TCNQ^-$ molecule has different redox property from the free $TCNQ^-$ and might be reduced to $TCNQ^{2-}$ by the reaction with $[Mn^{III}(salen)]^+$. However, the reduction potential of $TCNQ^-$ to $TCNQ^{2-}$ is much more negative compared with oxidation potential of Mn^{III} to Mn^{IV}, so the possibility (ii) can be excluded.

In the case of $[Fe^{II}(CH_3OH)_4(TCNQ)_2]TCNQ{\cdot}2CH_3CN$ (**2**), we prepared **2** from ferric species which has chemical formula $[Fe^{III}(salen)]^+$ in methanol solution. $TCNQ^-$ can not reduce the $[Fe^{III}(salen)]$ to iron(II) form from the electrochemical view point. It can be assumed that the redox properties of coordination compound like $[Fe^{III}(salen)(TCNQ)]$ are quite different from free ions. For example, oxidation potential of $TCNQ^-$ becomes more negative upon coordination to the metal ion, while reduction potential of $[Fe^{III}(salen)]^+$ becomes more positive upon coordination of $TCNQ^-$. This might make the formation of iron(II) and $TCNQ^0$ species possible in **2**.

Magnetic Properties. Magnetic susceptibilities of **1** and **2** were measured down to 6 K and $1/\chi_m$ vs. temperature plots are depicted in Fig. 5, where χ_m is molar susceptibility and the χ_m values for **1** are calculated for $[Mn(salen)(TCNQ)_{1/2}](CH_3OH)$. Temperature dependencies of $1/\chi_m$ values obey Curie–Weiss law, and Curie constant and Weiss temperature are respectively estimated to be 2.75 $emu\,K\,mol^{-1}$, −0.69 K for **1** and 3.24 $emu\,K\,mol^{-1}$, −3.15 K for **2**. The Curie constants for **1** and **2** are close to the value (3.0 $emu\,K\,mol^{-1}$) calculated with spin only equation (S=2 and g=2.00). The magnetic behaviors for **1** and **2** lead to conclude that the magnetic interaction between metal centers are very small and the $TCNQ^-$ anions in **2** form a diamagnetic dimer (or column). Deviation of the observed Curie constants from the spin only value can be explained by an orbital contribution to the magnetic moments.[21)] Mn^{III} and Fe^{II} ions in **1** and **2** have d^4 (^5E state) and d^6 (^5T state) electronic configurations, respectively, so both metal ions have four spins (S=2 states). Fe^{II} ions has an orbital angular moment.

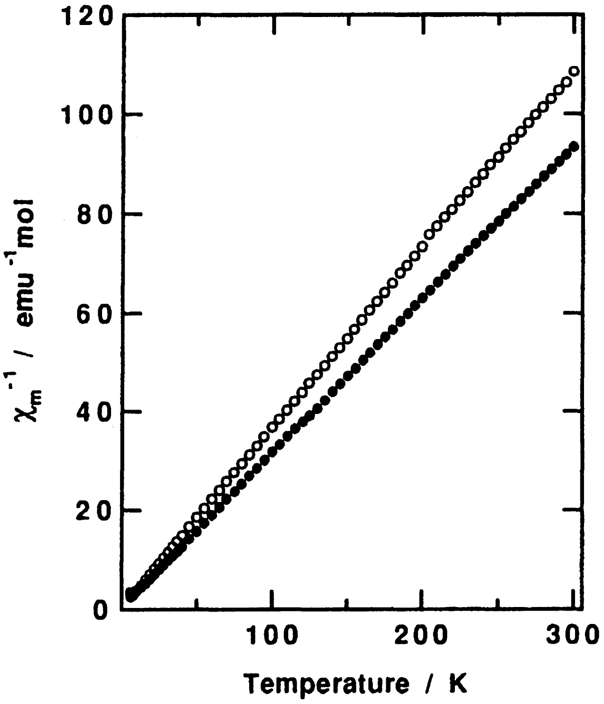

Fig. 5. $1/\chi_m$ vs. T plots of (●) $[Mn^{III}(salen)(TCNQ)_{0.5}][Mn^{III}(salen)(TCNQ)_{0.5}(CH_3OH)]CH_3OH{\cdot}H_2O$ (**1**) and (○) $[Fe^{II}(CH_3OH)_4(TCNQ)_2]TCNQ{\cdot}2CH_3CN$ (**2**).

Mn^{III} ion (^5E) has no orbital angular momentum, however, this term can mix with the higher lying $^5T_2$ term. Therefore, the orbital contributions should be included in interpretation of the magnetic properties for Fe^{II} and Mn^{III} ions. Observed magnetic momentum can be expressed as follows:

$$\mu = \mu_{\text{s.o.}} \left(1 - \frac{\alpha\lambda}{10\,Dq}\right),$$

where $\mu_{\text{s.o.}}$, α, λ, and Dq represent spin only magnetic moment, general parameter, spin-orbit coupling constant, and crystal field parameter, respectively. The spin orbit coupling constants for Mn^{III} (d^4) and Fe^{II} (d^6) ions are positive and negative, respectively. Therefore, the observed Curie constants for Mn^{III} and Fe^{II} ions are respectively larger and smaller than the spin-only value, and this is in accord with the experimental results.

Conclusion

The structure of $[Mn^{III}(salen)(TCNQ)_{0.5}][Mn^{III}(salen)(TCNQ)_{0.5}(CH_3OH)]CH_3OH{\cdot}H_2O$ (**1**) presents one of the rare examples of metal complexes with $TCNQ^{2-}$ and $TCNQ^{2-}$ bridges Mn^{III} chromophores in μ_2- and μ_4-fashions to form one dimensional chain. $[Fe^{II}(CH_3OH)_4(TCNQ)_2]TCNQ{\cdot}2CH_3CN$ (**2**) has two dimensional network, where $TCNQ^0$-$TCNQ^-$ columns were linked by the iron(II) chromophores. Electrochemical measurements suggest that redox properties of compounds might change upon coordination and unexpected redox reactions might occurs to form unusual oxidation states in the compounds. Magnetic susceptibility measurement showed the very small antiferromagnetic interactions between metal centers in **1** and **2**.

It is important to know which paramagnetic metal ions can interact with each other through organic radicals, when new magnetic materials are designed. Present and our previous results$^{12)}$ lead to conclude that Mn^{III} (d^4), Mn^{II} (d^5), and Fe^{II} (d^6) ions seems not to be a good candidate for network constituents. It can be suggested that possibilities of the second and third transition metal ions as a network constituents should be explored.

This work was in part supported by a Grant-in-Aid for Scientific Research on Priority Area "Molecular Magnetism" (Area No. 228/No. 06218203) and No. 05453039 from Ministry of Education, Science and Culture. Financial support by the Kurata Foundation is gratefully acknowledged.

References

1) J. S. Miller and A. J. Epstein, *Angew. Chem., Int. Ed. Engl.*, **33**, 385 (1994).

2) J. S. Miller, J. C. Calabrese, H. Rommelmann, S. Chittapeddi, J. H. Zhang, W. M. Reiff, and A. J. Epstein, *J. Am. Chem. Soc.*, **109**, 769 (1987).

3) G. T. Yee, J. M. Manriquez, D. A. Dixson, R. S. MacLean, D. M. Groski, R. B. Flippen, K. S. Narayan, A. J. Epstein, and J. S. Miller, *Adv. Mater.*, **3**, 309 (1991).

4) P. Zhou, M. Makivic, F. Zuo, S. Zane, J. S. Miller, and A. J. Epstein, *Phys. Rev. B*, **49**, 4367 (1994).

5) G. A. Candera, L. J. Swartzendruber, J. S. Miller, A. H. Rice, L. D. Prestone, J. M. Williams, S. W. Peterson, and M. J. Rice, *J. Am. Chem. Soc.*, **101**, 2755 (1979).

6) W. E. Broderick, J. A. Thompson, E. P. Day, and B. M. Hoffman, *Science*, **249**, 401 (1990).

7) W. E. Broderick and B. M. Hoffman, *J. Am. Chem. Soc.*, **113**, 6334 (1991).

8) J. M. Manriquez, G. T. Yee, R. S. McLean, A. J. Epstein, and J. S. Miller, *Science*, **252**, 1415 (1991).

9) C. Kollmar and O. Kahn, *Acc. Chem. Res.*, **26**, 259 (1993).

10) J. P. Cornelissen, J. H. van Diemen, L. R. Groeneveld, J. G. Haasnoot, A. L. Spek, J. Reedijk, *Inorg. Chem.*, **31**, 198 (1992).

11) P. Lacroix, O. Kahn, A. Gleizes, L. Valade, and P. Cassoux, *Nouv. J. Chim.*, **8**, 643 (1984).

12) H. Oshio, E. Ino, I. Mogi, and T. Ito, *Inorg. Chem.*, **32**, 5697 (1993).

13) G. C. Dailey, C. P. Horwitz, and C. A. Lisek, *Inorg. Chem.*, **31**, 5325 (1992).

14) "Theory and Application of Molecular Paramagnetism," ed by E. A. Boudreaux and L. N. Mulay, Wiley and Sons, Inc., New York (1976).

15) G. M. Sheldrick, "SHELXS-86," University of Göttingen, Germany (1986).

16) S. R. Hall and J. M. Sterwart, "XTAL3.2,"

Universities of Western Australia and Maryland, Nedlands, Australia, and College Park, MD (1992).

17) a) J. S. Miller, J. H. Zhang, W. M. Reiff, D. A. Dixson, L. D. Preston, A. H. Reis, E. Gebert, M. Extine, J. Troup, A. J. Epstein, and M. D. Ward, *J. Phys. Chem.*, **91**, 4344 (1987); b) D. B. Tanner and C. S. Jacobsenmm, *Mol. Cryst. Liq. Cryst.*, **85**, 137 (1982); c) M. Inoue and M. B. Inoue, *J. Chem. Soc., Faraday Trans.*, **81**, 539 (1985); d) D. G. Humphrey, G. D. Fallon, and K. S. Murray, *J. Chem. Soc., Chem. Commum.*, **1988**, 1356; e) J. S. Miller, private Communication.

18) A. Girlando and C. Pecile, *Spectrochim. Acta, Part A*, **29A**, 1859 (1973).

19) M. S. Khatkale and J. P. Devlin, *J. Chem. Phys.*, **70**, 1851 (1979).

20) H. Endres, "Extended Linear Chain Compounds," ed by J. S. Miller, Plenum Press, New York (1983), Vol. 3, p. 263.

21) "Magnetism and Transition Metal Complexes," ed by F. E. Mubbs and D. J. Machin, Wiley and Sons, Inc., New York (1973).

22) a) R. E. Long, R. A. Sparks, and K. N. Truebblood, *Crystallogr.*, **B30**, 932 (1965); b) P. Cassoux and A. Gleizes, *Inorg. Chem.*, **19**, 665 (1980); c) N. Matsumoto, T. Miyazaki, Y. Sagara, and A. Ohyoshi, *Inorg. Chim. Acta*, **63**, 249 (1982); d) N. Matsumoto, Y. Nonaka, and S. Kida, *Inorg. Chim. Acta*, **37**, 27 (1979); e) P. Bergamini, V. Bertolasi, V. Ferretti, and S. Sostero, *Inorg. Chim. Acta*, **126**, 151 (1987); f) J. J. Mayerle, *Inorg. Chem.*, **16**, 916 (1977); g) L. J. Pace, A. Ulman, and J. A. Ibers, *Inorg. Chem.*, **21**, 199 (1982).

23) a) A. Bencini and C. Zanchini, *Inorg. Chem.*, **30**, 4245 (1991); b) J. S. Miller, D. T. Gletzhofer, D. M. O'Hare, W. M. Reiff, A. Chakraborty, and A. J. Epstein, *Inorg. Chem.*, **28**, 2930 (1989); c) D. H. Endres, H. J. Keller, W. Moroni, and D. Nöthe, *Acta. Crystallogr., Sect. B*, **B33**, 2428 (1977); d) Y. Saito and M. Konno, *Acta Crystallogr., Sect. B*, **B31**, 2007 (1975).